



THE UNIVERSITY *of* EDINBURGH

Edinburgh Research Explorer

## Strength characterisation of soil-based construction materials

**Citation for published version:**

Beckett, C, Augarde, CE, Easton, D & Easton, T 2017, 'Strength characterisation of soil-based construction materials', *Geotechnique*, vol. 68, no. 5, pp. 400-409. <https://doi.org/10.1680/jgeot.16.P.288>

**Digital Object Identifier (DOI):**

[10.1680/jgeot.16.P.288](https://doi.org/10.1680/jgeot.16.P.288)

**Link:**

[Link to publication record in Edinburgh Research Explorer](#)

**Document Version:**

Peer reviewed version

**Published In:**

Geotechnique

**General rights**

Copyright for the publications made accessible via the Edinburgh Research Explorer is retained by the author(s) and / or other copyright owners and it is a condition of accessing these publications that users recognise and abide by the legal requirements associated with these rights.

**Take down policy**

The University of Edinburgh has made every reasonable effort to ensure that Edinburgh Research Explorer content complies with UK legislation. If you believe that the public display of this file breaches copyright please contact [openaccess@ed.ac.uk](mailto:openaccess@ed.ac.uk) providing details, and we will remove access to the work immediately and investigate your claim.



# Strength characterisation of soil-based construction materials

C.T.S. Beckett<sup>a</sup>, C.E. Augarde<sup>b</sup>, D. Easton<sup>c</sup>, T. Easton<sup>c</sup>

<sup>a</sup>*School of Civil, Environmental and Mining Engineering, University of Western Australia, Perth, WA 6009*

<sup>b</sup>*School of Engineering and Computing Sciences, Durham University, Durham, DH1 3LE, UK*

<sup>c</sup>*Watershed Materials, 11 Basalt Road, Napa, CA 94558, USA*

---

## Abstract

Rammed earth (RE) is a venerable construction technique, gaining attention today due to its environmental and sustainable qualities. A key obstacle to its wider adoption is a lack of strength characterisation methods to aid in design and conservation. Research over the past decade has demonstrated that suction is the key mechanism behind strength and strength gain. As suction changes with the building's environment, being able to predict strength changes with suction is essential for practitioners and conservators alike. This paper presents a method for predicting RE strengths based on the Extended Mohr Coulomb (EMC) framework. Construction of an EMC failure envelope in the residual suction range is discussed and the use of a planar envelope justified. Unconfined compression and indirect tensile tests on two RE soils are used to construct this envelope and methods to predict strengths from it are derived. Excellent agreement between measured and predicted strengths is also found for available literature data. Simplifications are identified to adapt the developed technique to suit RE practice and a suitable experimental procedure is outlined. Finally, the revised experimental procedure is employed at an existing RE construction facility to successfully predict strengths of a compacted Californian sandy loam.

*Keywords:* Rammed earth, suction, Extended Mohr-Coulomb, climate change

---

## 1 1. Introduction

2 Although the ancient practice of rammed earth (RE) has been demonstrably  
3 successful for millennia, the global renaissance of this venerable technique, which  
4 is currently underway across the globe, has been hampered by the imposition of  
5 engineering standards that are more appropriate to reinforced concrete. In order  
6 to secure building code compliance, RE practitioners find themselves required  
7 to attain compressive strengths for their installed wall systems (e.g. NZS 4297,  
8 Walker and Standards Australia (2002)) that are usually beyond those achievable  
9 for soil-based masonry unless Portland cement or other CO<sub>2</sub> generating stabilizers  
10 are used to augment the clay-based aggregates.

11 Clearly, history demonstrates durability for RE that contradicts the strength  
12 requirements currently mandated. The RE industry, albeit a small fraction of  
13 the more conventional cement-based masonry industry, can benefit from a set of  
14 testing protocols that will establish a new set of limits (or standards) from which  
15 the testing and permitting agencies can align with the practitioners. Given that  
16 unstabilised RE is far more susceptible to strength loss at saturation than sta-  
17 bilized rammed earth, a thorough understanding of the mechanisms that govern  
18 strength gain and strength loss in clay-based aggregates is critical to the ultimate  
19 success of the industry. Concurrently, RE and other earthen buildings represent  
20 a significant proportion of our built heritage. Maintaining this heritage demands  
21 a scientific approach to predict and forecast material properties. Therefore, this

---

*Email addresses:* [christopher.beckett@uwa.edu.au](mailto:christopher.beckett@uwa.edu.au) (C.T.S. Beckett),  
[charles.augarde@dur.ac.uk](mailto:charles.augarde@dur.ac.uk) (C.E. Augarde), [david@watershedmaterials.com](mailto:david@watershedmaterials.com) (D. Easton),  
[taj@watershedmaterials.com](mailto:taj@watershedmaterials.com) (T. Easton)

22 paper sets out to: i) experimentally examine RE strength variation through a  
23 comprehensive experimental campaign; ii) develop a framework to predict RE  
24 strength change given known environmental conditions; iii) adapt that frame-  
25 work to devise a series of characterisation tests sufficiently simple to be useful for  
26 practice.

## 27 **2. Experimental programme**

28 Suction is a key factor responsible for developing RE's strength and the source  
29 of its ability to maintain, in effect, vertical 'slopes' for thousands of years. Un-  
30 derstanding the effects of suction variation is therefore critical to any attempt to  
31 characterise RE behaviour (Jaquin et al., 2009; Gerard et al., 2015). This sec-  
32 tion describes the experimental programme developed to investigate RE strength  
33 under controlled suction conditions.

### 34 *2.1. Materials*

35 Site soils can be highly variable and so are inconvenient for laboratory inves-  
36 tigation. Instead, 'engineered' soils, manufactured from known quantities of raw  
37 materials, were used in this study to guarantee mineralogical and grading con-  
38 sistency. Soils used in this investigation were selected to represent the range of  
39 materials used for RE construction around the world are listed in Table 1. Soils  
40 were named after their targeted constituent proportions; for example, Soil 4-5-1  
41 nominally comprised 40% silty clay ("Birtley" clay, LL 58.8%, PL 25.7%, 50%  
42 kaolinitic clay), 50% sand and 10% gravel by mass. Soils 4-5-1 and 2-7-1 com-  
43 prised the maximum and minimum recommended silty clay ( $\leq 60\mu\text{m}$ ) contents for  
44 RE materials respectively (Houben and Guillaud, 1996), to investigate behaviour  
45 at the extreme material boundaries. Both soils had the minimum recommended

Table 1: Soil mix constituents, OWC and  $\rho_{d,max}$

Soil	Clay (%)	Silt (%)	Sand (%)	Gravel (%)	OWC (%)	$\rho_{d,max}$ (kg/m <sup>3</sup> )
4-5-1	19.9	17.2	52.7	10.2	12.0	1940
2-7-1	9.9	9.5	70.7	9.9	12.0	1960

46 gravel contents (10%) to reduce the influence of large particles on test results and  
 47 are considered sandy loams by the USDA classification system. Grading curves  
 48 are given in Figure 1. Soil optimum water contents (OWCs) and maximum dry  
 49 densities ( $\rho_{d,max}$ ) were determined using the Standard Proctor Test (BS 1377),  
 50 also given in Table 1.

51 (Insert Figure 1 somewhere near here)

## 52 2.2. Strength testing

53 The Vapour Equilibrium (VE) method was used to control suction during  
 54 testing by equilibrating specimens to set temperatures ( $T$ ) and relative humidities  
 55 (RH). Under equilibrium conditions, total suction,  $\psi_t$ , is controlled by  $T$  and RH  
 56 according to the Kelvin Equation:

$$\psi_t = -\frac{R_u T}{v_m} \ln(\text{RH}) \quad (1)$$

57 where  $R_u$  is the universal gas constant (8.314 J/molK) and  $v_m$  is the molar volume  
 58 of pure water ( $18.016 \times 10^{-6}$  m<sup>3</sup>/mol). Suction is highly sensitive to seemingly  
 59 minor changes in atmospheric conditions; by Eqn 1, reducing RH from 70% to  
 60 50% at 20°C increases suction from 48.3 to 93.8 MPa.

61 Strengths at different suction values were examined using a combination of  
 62 unconfined compression (UCS) and indirect tensile (ITS) testing. UCS is com-  
 63 monly used to compare the performance of different RE soils and so is a technique

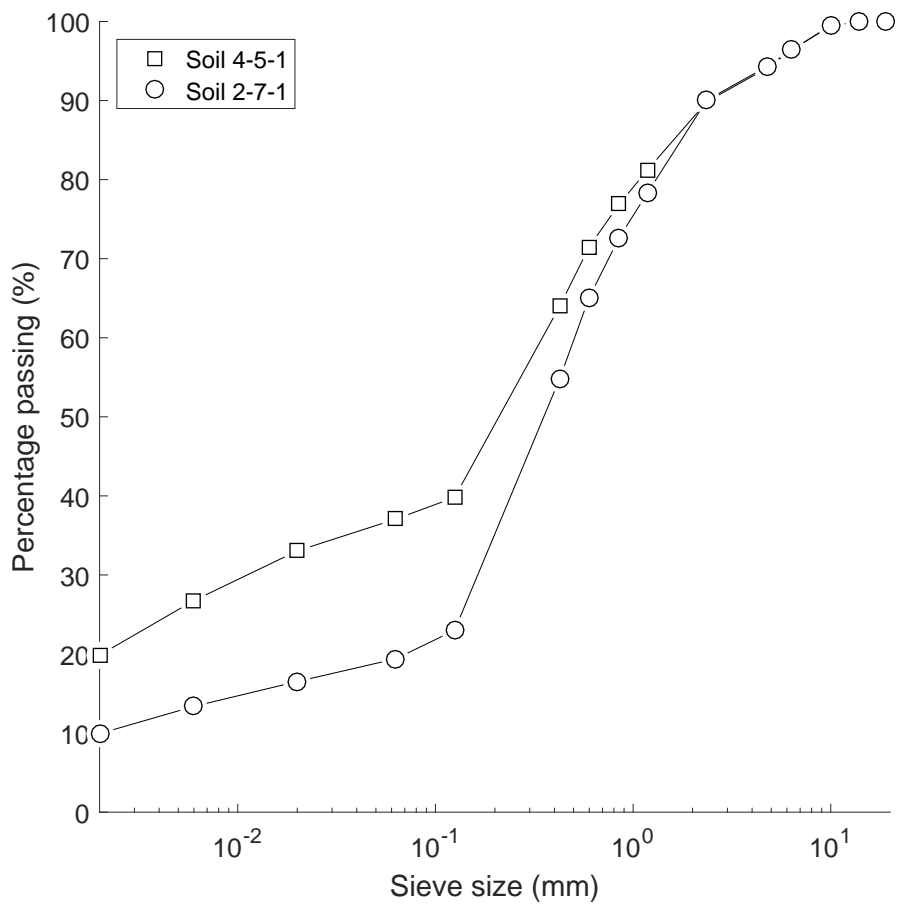


Figure 1: Particle grading curves for mixes 4-5-1 and 2-7-1

64 already familiar to RE practitioners. ITS was selected as specimen manufacture,  
65 handling and testing procedures are similar to those used for UCS testing and  
66 so can be accommodated by practitioners' existing facilities and expertise. ITS  
67 testing was previously reported in Beckett et al. (2015) but is briefly discussed  
68 here for convenience.

### 69 2.2.1. UCS testing

70 100mm cube specimens were manufactured for UCS testing. Although it is  
71 common to use  $\varnothing 100 \times 200$ mm cylindrical specimens, the smaller cube specimens  
72 were selected to reduce the amount of material needed. UCS specimens were  
73 manufactured at the OWC (using deionised water) and to  $\rho_{d,max}$  for that mix  
74 (Table 1) by compacting three equal layers of known mass to a controlled vol-  
75 ume. The upper surface of the specimen was scraped and depressions filled with  
76 a screed of fine material (parent soil sieved to pass 0.450mm) to ensure a level  
77 surface; this was necessary as specimens could not be rotated to present level  
78 surfaces, as is done when testing concrete. Specimens were removed from the  
79 mould immediately following manufacture and left to dry on wire racks under  
80 conditions of  $20 \pm 2^\circ\text{C}$  and  $45 \pm 15\%$  RH until reaching a constant mass for two  
81 consecutive days. Specimens were then equilibrated to RH=30, 50, 70 or 90%  
82 ( $\pm 3\%$ ) and  $T = 15, 20, 30$  or  $40^\circ\text{C}$  ( $\pm 2^\circ\text{C}$ ) (14–174MPa suction by Eqn 1) us-  
83 ing an environmental chamber (EC, Vötsch VC4033). An initial drying period  
84 was necessary prior to equilibration due to limited EC availability and difficul-  
85 ties in transporting fresh specimens. Specimens therefore either gained or lost  
86 water to achieve their final equilibration: consequences of testing specimens un-  
87 der wetting or drying conditions are discussed in the following sections. Once  
88 equilibrated, specimens were immediately transferred to a testing machine and

89 uniaxially loaded at a controlled displacement rate of 0.5mm/min until failure.  
90 Specimens were not capped as surfaces were level. Specimen water contents were  
91 determined by oven drying crushed material. Three specimens were manufac-  
92 tured per RH and  $T$  combination per soil; 96 in total.

93 RH and  $T$  values were selected to be representative of typical atmospheric  
94 conditions at RE sites around the world (Beckett and Augarde, 2012). How-  
95 ever, moisture contents can also be affected by incident rainfall or capillary rise  
96 (Hall and Djerbib, 2004). Under such circumstances, suction values are likely  
97 to fall below those examined here. However, these events constitute failures of  
98 the structural design, so that material would not be exposed to such conditions  
99 under normal circumstances. Consequences of suctions falling significantly below  
100 examined levels are discussed in the following sections. It should also be noted  
101 that UCS specimens behaved as soil elements due to equilibration to constant  
102 suction conditions. In practice, water content gradients may exist through RE  
103 structural components due to hygrothermal interactions with the surrounding  
104 atmosphere (McGregor et al., 2015). As such, our testing programme was not  
105 representative of *structural* element behaviour but can be used to assess potential  
106 strength changes along a moisture or suction gradient.

### 107 2.2.2. ITS testing

108  $\varnothing 100 \times 50$ mm ‘disc’ specimens were manufactured following a similar proce-  
109 dure to that for UCS specimens. Specimens were removed from the mould and  
110 air-dried on wire racks to a target water content, then wrapped in clear plastic  
111 for a minimum of two days for suction equilibration. Specimens were tested to  
112 failure at a displacement rate of 0.2mm/min between curved metal platens. Man-  
113 ufacturing and orientating specimens in this way tested indirect tensile strength



114 perpendicular to the compaction planes (Beckett et al., 2015). Tensile strength,  
115  $\sigma_t$ , was determined via

$$\sigma_t = -\frac{P}{\pi RL} \quad (2)$$

116 where  $P$  is the applied compressive load and  $R$  and  $L$  are the specimen radius  
117 and length respectively. Eqn 2 is valid for specimens with little deformation  
118 (Frydman, 1964). The highest suctions achieved from air-drying ITS specimens  
119 were 60 and 80 MPa for Soils 4-5-1 and 2-7-1 respectively. The minimum suction  
120 was roughly 1 MPa for both soils. Again, ITS testing was representative of soil,  
121 rather than structural, elements.

### 122 *2.3. Soil water retention properties*

123 Soil-water retention properties for Soils 4-5-1 and 2-7-1 were reported in Beck-  
124 ett et al. (2015). For convenience, the procedures used are briefly discussed here.  
125 Drying retention properties were determined using a combination of filter paper  
126 (suctions 0 to 4 MPa) and vapour-equilibrium (10 to 200 MPa) methods. Filter  
127 paper testing followed ASTM D5298-10. The relationship

$$\ln \psi_t = -4.6234 - 3.6454 \ln(w_{fp}) \quad (3)$$

128 was used to calculate  $\psi_t$  from the gravimetric water contents ( $w_{fp}$ ) of suspended  
129 filter papers (i.e. those in equilibrium with the surrounding air), determined via  
130 a best-fit relationship to data presented in Hamblin (1981). Soil water retention

131 curves (SWRCs) for each mix are shown in Figure 2, where data were fitted using

$$C = \left( 1 + \frac{\log\left(1 + \frac{\psi_t}{10^9}\right)}{\log(2)} \right) \quad (4)$$

$$S_r = C \times \frac{1}{\left( \ln\left(\epsilon + \left(\frac{\psi_t}{a}\right)^n\right) \right)^m} \quad (5)$$

132 where  $S_r$  is the degree of saturation,  $\epsilon$  is the Euler number,  $C$  is a correction term  
133 limiting  $S_r$  to 0 at  $\psi_t = 1\text{GPa}$  and  $a$ ,  $m$  and  $n$  are fitting parameters given in  
134 Figure 2 (Fredlund and Xing, 1994). Residual suction values ( $\psi_{res}$ ) were found  
135 from intersecting lines drawn tangentially to the steepest and shallowest parts  
136 of the curve. Although it is common to impose that the latter tangent passes  
137 through  $S_r = 0$  at  $\psi_t = 1\text{GPa}$ , the correction term in Eqn 5 causes bimodality  
138 in the high suction portion of the SWRC, producing an unrealistic estimation of  
139  $\psi_{res}$ ; tangents to the shallowest section of the curve were therefore used.  $\psi_{res}$   
140 and  $S_{r,res}$  are given in Figure 2.

141 (Insert Figure 2 somewhere near here)

### 142 3. Experimental results

143 UCS values for Soils 4-5-1 and 2-7-1 are shown in Figures 3 and 4 respectively.  
144 Note that UCS was not factored to account for the use of cubic, rather than the  
145 more common cylindrical, specimens. ITS results for untreated Soils 4-5-1 and  
146 2-7-1 from Beckett et al. (2015) are shown in Figure 5.

147 Figures 3 to 5 show that UCS roughly doubled and ITS increased tenfold  
148 between the lowest and highest tested suction conditions for both soils. It is  
149 possible that an RE structure might experience the full range of these conditions  
150 over the course of a single year; given their large surface area, equilibration to such

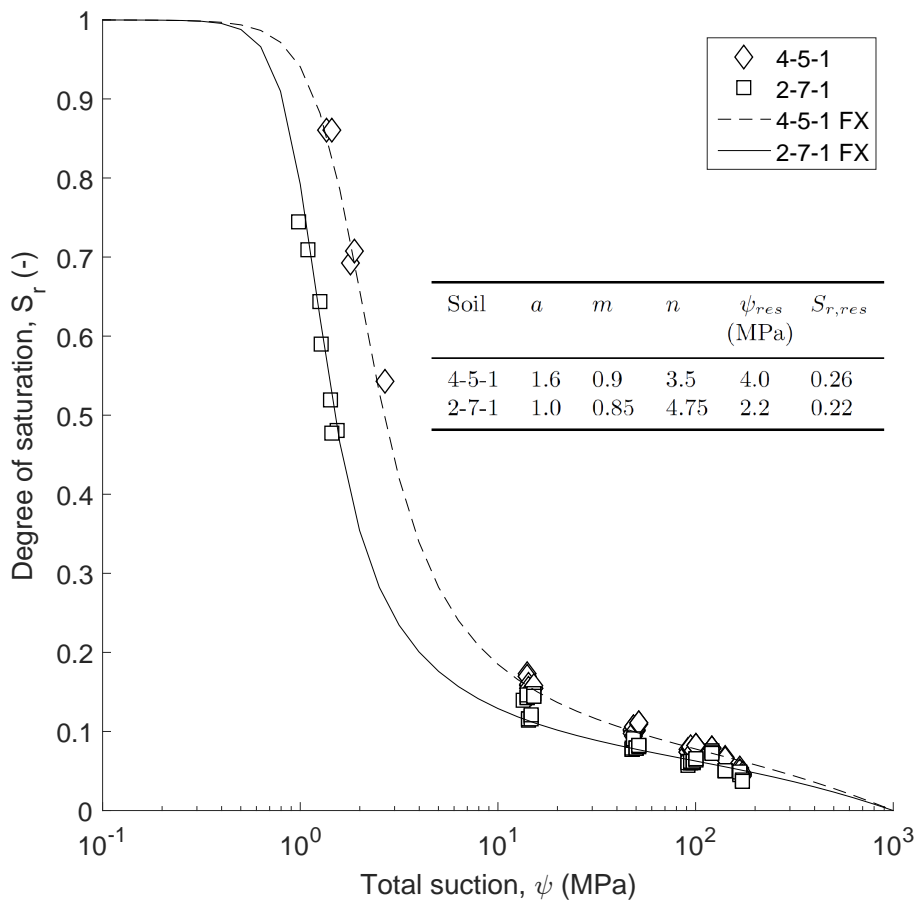


Figure 2: Soil 4-5-1 and 2-7-1 drying retention curves and fitting parameters. FX: fit using Eqn 5

151 conditions is rapid and large changes in strength over a building's life may result.  
152 Suction variation must therefore form the basis of any strength characterisation  
153 methods. The development of such a method is discussed in the following sections.

154 (Insert Figure 3 somewhere near here)

155 (Insert Figure 4 somewhere near here)

156 (Insert Figure 5 somewhere near here)

## 157 4. Constitutive model development

### 158 4.1. Extended Mohr-Coulomb failure criterion in the residual suction range

159 Two common approaches exist to incorporate suction into an effective stress  
160 framework. The generalised effective stress method uses an effective stress pa-  
161 rameter,  $\chi$ , to modify the existing pore water pressure term:

$$\sigma' = \sigma - \chi(u_a - u_w) \quad (6)$$

162 where  $u_a$  and  $u_w$  are the pore air and water pressures respectively. The advantage  
163 of Eqn 6 is that it is similar in construction to the Terzaghi effective stress  
164 approach familiar to most geotechnical engineers. However, the form of  $\chi$  is  
165 disputed and heavily dependent on the form of the SWRC (Khalili and Khabbaz,  
166 1998). An alternative to this approach is to introduce suction as a third stress  
167 state variable (Fredlund and Morgenstern, 1977). Shear strength is calculated  
168 via

$$\tau_f = c' + (\sigma - u_a) \tan \phi + (u_a - u_w) \tan \phi^b \quad (7)$$

169 where  $c'$  is the effective cohesion,  $\phi'$  is the effective friction angle and  $\tan \phi^b$   
170 describes the change in shear strength with suction at a constant value of net

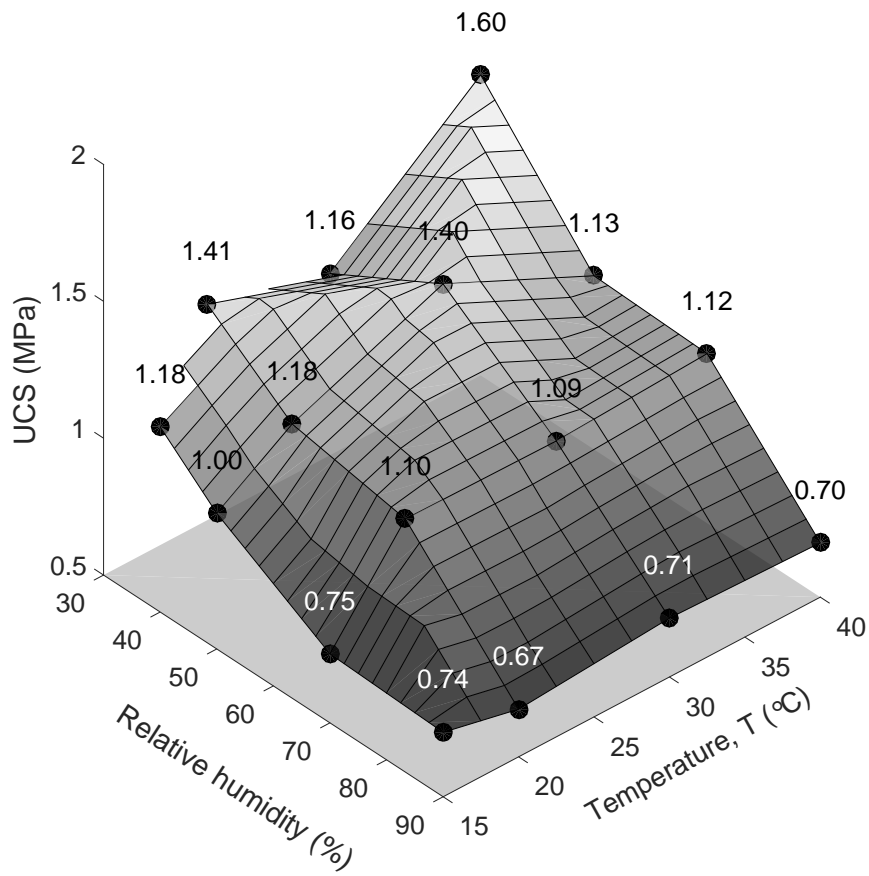


Figure 3: UCS results for Soil 4-5-1 (individual values shown above markers)

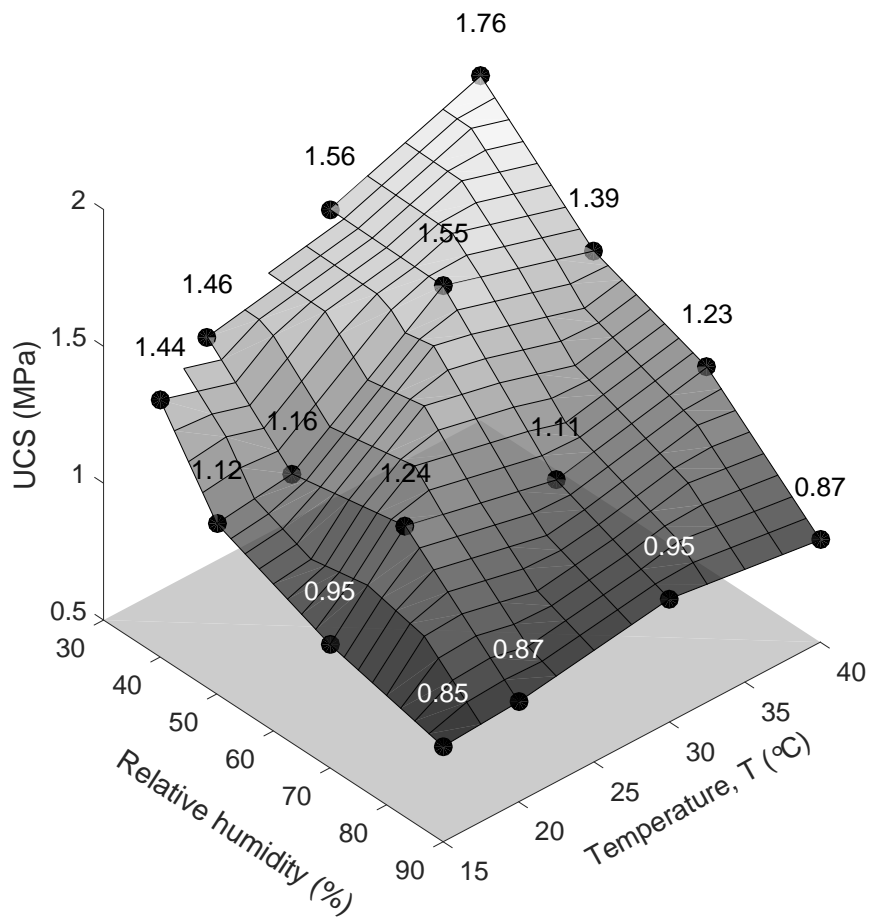


Figure 4: UCS results for Soil 2-7-1 (individual values shown above markers)

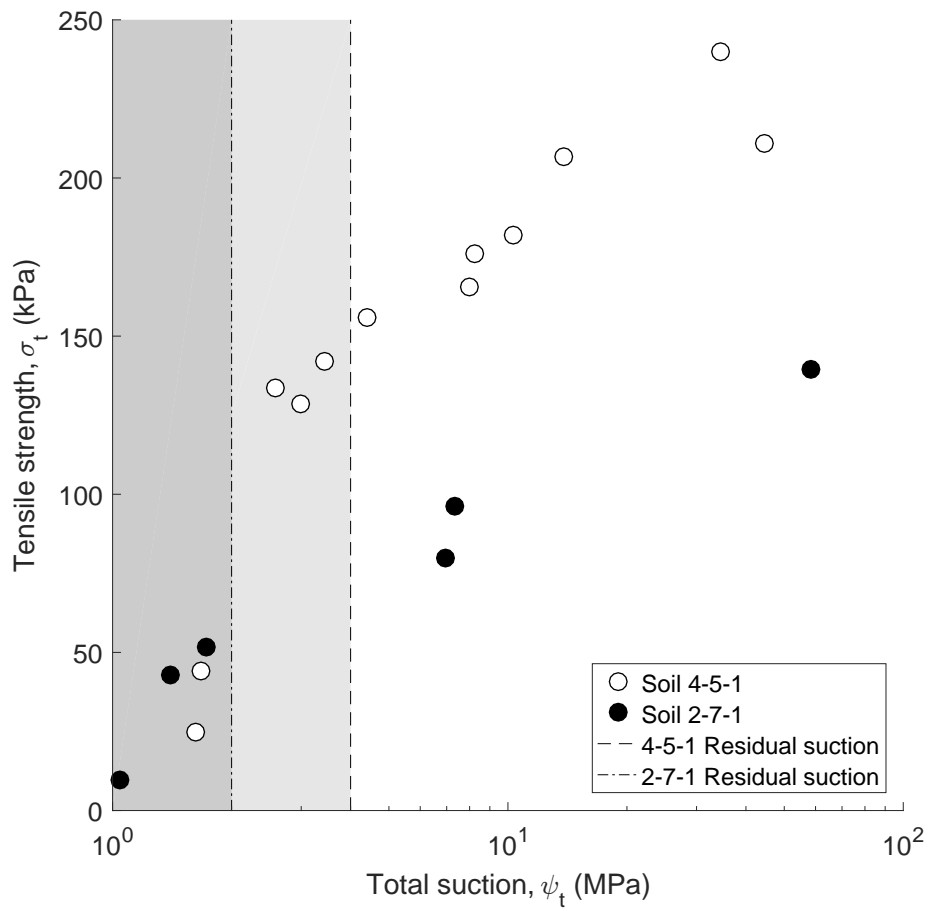


Figure 5: ITS results for Soils 4-5-1 and 2-7-1 from Beckett et al. (2015). Shaded regions show suctions below residual values

171 stress ( $\sigma - u_a$ ). It is generally accepted that  $\phi^b$  is a function of  $S_r$  and diminishes  
 172 to small values as  $S_r$  approaches zero (Gan et al., 1988; Fredlund and Rahardjo,  
 173 1993). The advantage of this “extended” Mohr-Coulomb criterion (EMC) is that  
 174 the contributions of suction and net stress can be assessed separately.

175  $\phi'$  is commonly assumed to be constant in the residual suction range (Fredlund  
 176 et al., 1987). However, the form of  $\phi^b$  depends on the range of suction investi-  
 177 gated. Fredlund et al. (1996) and Vanapalli et al. (1996) presented a method to  
 178 predict values of  $\phi^b$  from  $\phi'$  for given values of suction, via

$$\tan \phi^b = \left( \Theta(\psi)^\kappa + \psi \frac{d(\Theta(\psi)^\kappa)}{d\psi} \right) \tan \phi' \quad (8)$$

179 where  $\Theta = \frac{\theta(\psi) - \theta_{res}}{\theta_s - \theta_{res}}$ ,  $\theta(\psi)$ ,  $\theta_s$  and  $\theta_{res}$  are the volumetric water contents at  
 180 the current, saturation and residual suction values respectively and  $\kappa$  is a fitting  
 181 parameter. As  $\Theta \leq 1 \forall \psi$ , Eqn 8 maintains  $\phi^b < \phi'$  for suctions above the air-  
 182 entry value as discussed above. To avoid negative values of  $\Theta$  for  $\theta < \theta_{res}$ , Eqn 8  
 183 can be simplified by assuming  $\theta_{res} = 0$  so that  $\Theta = S_r$ , i.e.

$$\tan \phi^b = \left( S_r(\psi)^\kappa + \psi \frac{d(S_r(\psi)^\kappa)}{d\psi} \right) \tan \phi'. \quad (9)$$

184 Depending on the expression used for the SWRC (e.g. Eqn 5),  $\frac{d(S_r^\kappa)}{d\psi}$  in Eqn 9 can  
 185 be quite complex. However, assuming a linear SWRC in the residual suction range  
 186 (as supported by Figure 2) reduces  $\frac{d(S_r(\psi)^\kappa)}{d\psi}$  to a constant value. As  $\frac{d(S_r(\psi)^\kappa)}{d\psi}$  is  
 187 small,  $S_r(\psi)^\kappa$  is also nominally constant. Therefore, in the residual suction range,  
 188 we assumed  $\phi^b$  to be constant and so the failure envelope to be planar.



Table 2: EMC parameters determined for RE soils

Soil	$c'$ (MPa)	$\phi'$ ( $^\circ$ )	$\phi^b$ ( $^\circ$ )	$\phi^b$ ( $^\circ$ , Eqn 9)	$\kappa$ (Eqn 9)	Fitted suction range (MPa)
4-5-1	0.24	24.5	0.082	0.084	1.25	4.0–60
2-7-1	0.15	39.7	0.093	0.092	1.44	4.0–80

189 *4.2. Modelling experimental data*

190 UCS data discussed above and ITS results for untreated material from Beckett  
 191 et al. (2015) were used to construct EMC failure surfaces for Soils 4-5-1 and  
 192 2-7-1. Construction of the failure envelope from UCS and ITS data is shown  
 193 schematically in Figure 6. The final fitted plane for 2-7-1 is shown in Figure 7.  
 194 Mohr’s circles for UCS tests were drawn assuming that  $\sigma_2 = \sigma_3 = 0$  and  $\sigma_1 = \sigma_c$ .  
 195 ITS Mohr’s circles were drawn assuming  $\sigma_2 = 0$ ,  $\sigma_3 = \sigma_t$  and  $\sigma_1 = -3\sigma_t$  (noting  
 196 that  $\sigma_t$  is negative in Eqn 2). ITS relationships were derived in Li and Wong  
 197 (2013) and are valid for specimens with little deformation, as is the case for such  
 198 high suction values. Circles were discretised and points for best plane fitting were  
 199 determined via a least squares approach. Planes were fitted using the suction  
 200 range for which both UCS and ITS data were available.  $c'$ ,  $\phi'$  and  $\phi^b$  and the  
 201 fitted suction range for each soil are given in Table 2.

202 (Insert Figure 6 somewhere near here)

203  $\phi'$  values in Table 2 were similar to those typically found for compacted sandy  
 204 loam soils, e.g. Vanapalli et al. (1996). Although  $\phi^b$  values were close to zero,  
 205 as expected for results in the residual suction range, the contribution of  $\phi^b$  to  
 206 strength was significant due to the high values of suction present.  $\kappa$  was selected  
 207 to produce the best match between experimental  $\phi^b$  values and those found via  
 208 Eqn 9 using experimentally-derived  $\phi'$  and SWRCs.  $\kappa$  fell within the  $\kappa = 1-3$  lim-  
 209 its suggested by Fredlund et al. (1996) for both soils, supporting the assumption

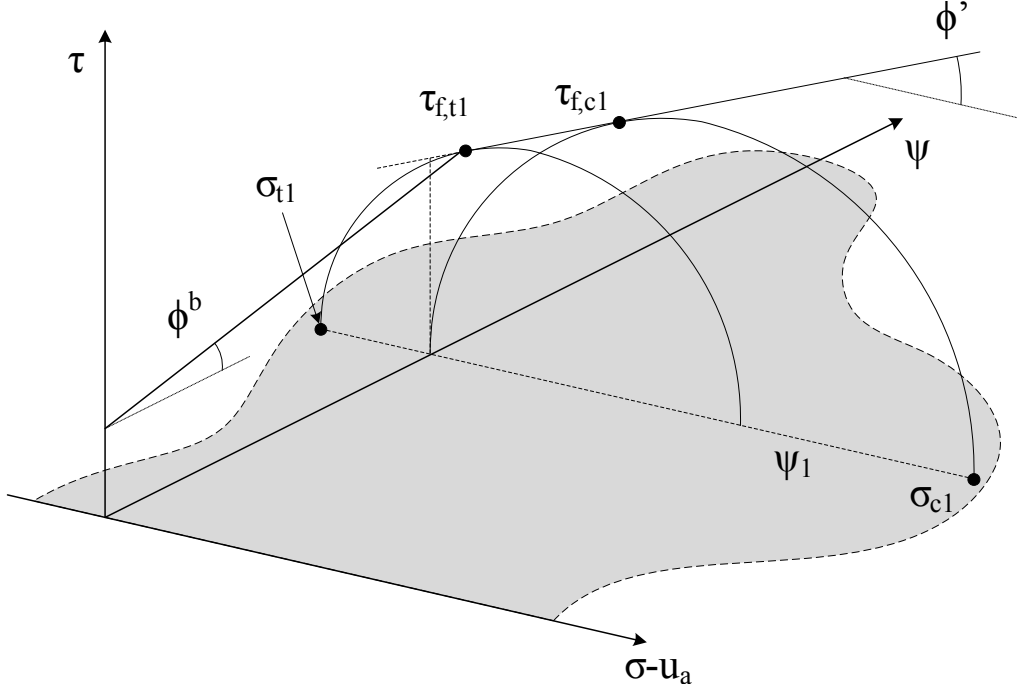


Figure 6: Construction of the planar EMC failure envelope using UCS and ITS data

210 of a planar failure envelope in the residual suction range. Although Soil 2-7-1  
 211 achieved a higher UCS for all tested suction values, the fitted plane had a lower  
 212  $c'$  value than for Soil 4-5-1; this was due to the poor performance of Soil 2-7-1  
 213 in tension. Soil 2-7-1's lower  $c'$  was countered by higher  $\phi'$  and  $\phi^b$  values. A  
 214 higher  $\phi'$  value was likely due to Soil 2-7-1's higher dry density and so greater  
 215 particle interlock. The higher  $\phi^b$  value was due to a shallower retention curve  
 216 in the residual range, diminishing the contribution of the term in parentheses  
 217 (negative) in Eqn 9.

218 (Insert Figure 7 somewhere near here)

219 UCS can be predicted from fitted  $c'$ ,  $\phi'$  and  $\phi^b$  values via

$$\text{UCS} = 2 \left( \frac{c' + \psi \tan \phi^b}{\cos \phi' - (1 - \sin \phi') \tan \phi'} \right) \quad (10)$$

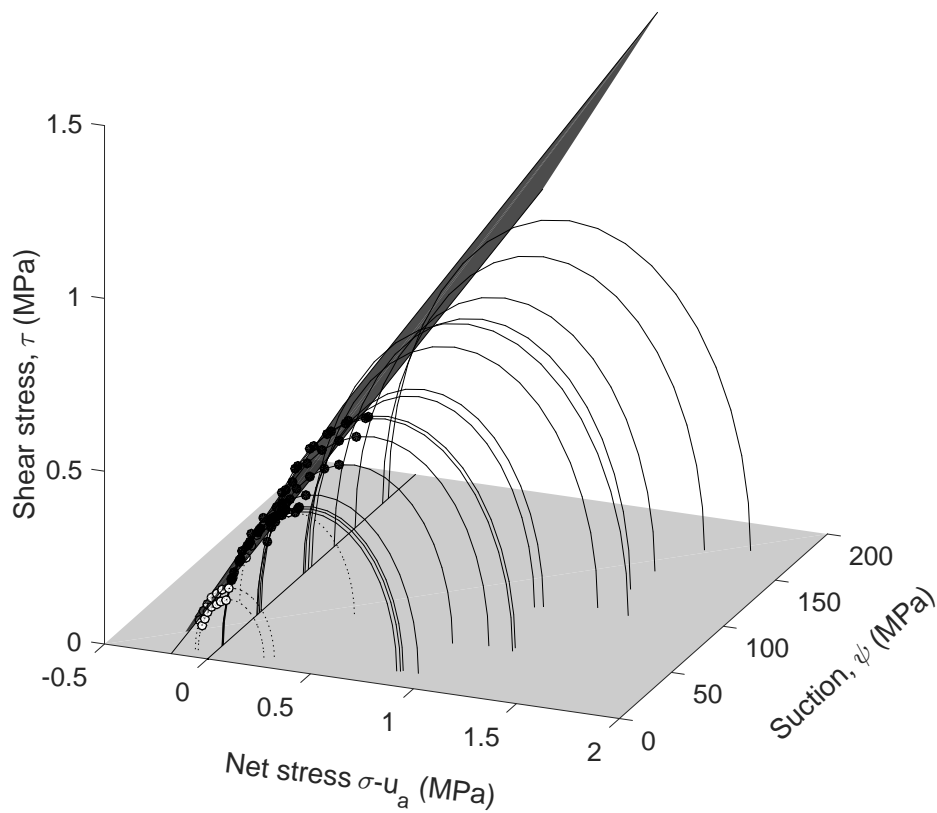


Figure 7: Soil 2-7-1 planar EMC failure envelope. - UCS results; - - ITS results. Markers denote points on the circles used for plane fitting. Mohr's circles without markers fell outside the ITS suction range

Eqn 10 is similar to that proposed by Panayiotopoulos (1996) to find UCS using the generalised effective stress approach, however it maintains a clear distinction between the suction (the numerator) and internal friction (the denominator) contributions to UCS. Figure 8 compares measured UCS values for mixes 4-5-1 and 2-7-1 and those predicted via Eqn 10. Predictions fall evenly about the line of equality ( $\pm 0.15$  MPa). Notably, there was no significant change in prediction accuracy for UCS values above the upper ITS suction limit (i.e. above the range for which plane fitting was defined) for either soil. Good accuracy beyond the fitted range was due to the near-linear SWRC for suctions above the residual value. Given the sensitivity of the SWRC gradient to the correction term in Eqn 5 in the residual range, it is likely that the quality of fit would reduce for suctions much higher than those tested. The fit quality would also suffer for suctions below the residual value, for example as might arise during capillary rise. However, for the range investigated, a planar failure envelope was suitable.

(Insert Figure 8 somewhere near here)

#### 4.3. Application to literature data

Few suction-dependent RE strength datasets are available in the literature. However, RE water retention and UCS data were presented in Jaquin et al. (2009), Bui et al. (2014) and Gerard et al. (2015). Properties of those soils are given in Table 9. Failure planes were fitted to Mohr's circles constructed from UCS and suction data in the residual suction range, as judged by SWRCs in those works, using the procedures discussed in the previous section. As only UCS data was available for data in Jaquin et al. (2009) and Bui et al. (2014), plane fitting was forcibly restricted to  $\phi', \phi^b > 0$ . The full procedure was implemented for data from Gerard et al. (2015).  $c', \phi'$  and  $\phi^b$  values for these soils are given in Table 4

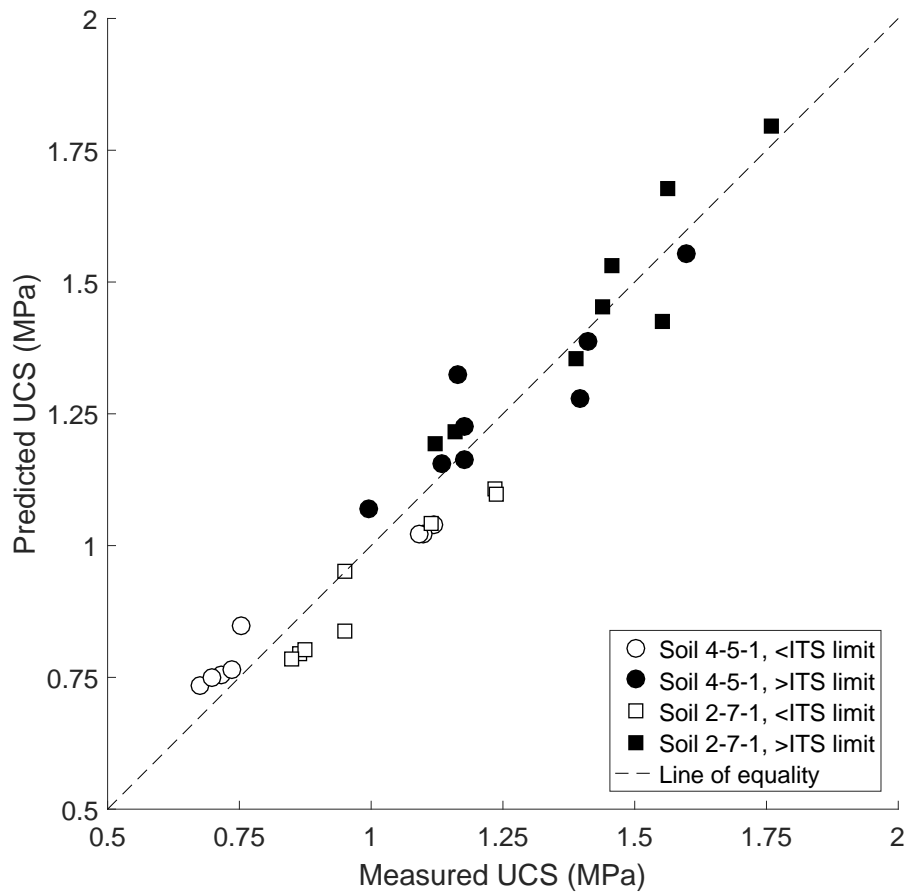


Figure 8: Comparison of measured and predicted UCS above and below ITS suction limit

Table 3: Constituents of soils used in the literature. CWC: Compaction Water Content. \*Stabilised with 2% natural hydraulic lime. \*\*Predominantly kaolinitic. \*\*\*Predominantly montmorillonitic

Soil	Clay (%)	Silt (%)	Sand (%)	Gravel (%)	CWC (%)	$\rho_{d,max}$ (kg/m <sup>3</sup> )
Jaquin et al. (2009)	—15**—		25	60	12	2040
Bui et al. (2014) Soil A	5***	30	49	16	11	1920
Bui et al. (2014) Soil B*	4***	35	59	2	11	1920
Bui et al. (2014) Soil C	9***	38	50	3	11	1920
Gerard et al. (2015)	13**	64	26	0	15	1840

245 and measured and predicted UCS values are compared in Figure 9.  $\phi^b$  values were  
246 larger than those in Table 2 due to the narrower fitted suction range. Excepting  
247 Bui et al. (2014) Soil C,  $\kappa$  values outside of the 1–3 limit were required to match  
248 experimental and predicted  $\phi^b$  values, most notably for Jaquin et al. (2009). By  
249 Eqn 9, a low  $\kappa$  value indicated little contribution of suction or saturation changes  
250 to changes in  $\phi^b$ , so that  $\phi^b \approx \phi'$  as is expected at low suction. That values  
251 marginally outside the 1–3 limit were needed to fit other soils is reasonable given  
252 the restriction to UCS results only for Bui et al. (2014) or the extremely high  
253 strengths found in Gerard et al. (2015). Notably, the fit quality was seemingly  
254 unaffected the presence of stabiliser (Bui et al. (2014) Soil B); this was perhaps  
255 to be expected, given the low stabiliser and clay contents (for lime, the latter  
256 is required for the former to react) and the strong contribution of suction to  
257 strength for weakly lime-stabilised RE (Ciancio et al., 2014).

258 (Insert Figure 9 somewhere near here)

## 259 5. Adaptation to practice

260 At present, RE construction is hampered by a lack of construction codes or  
261 standards and a shallow pool of available contractors. It is therefore unrealistic to  
262 assume that RE practitioners can perform a wide range tests for every potential

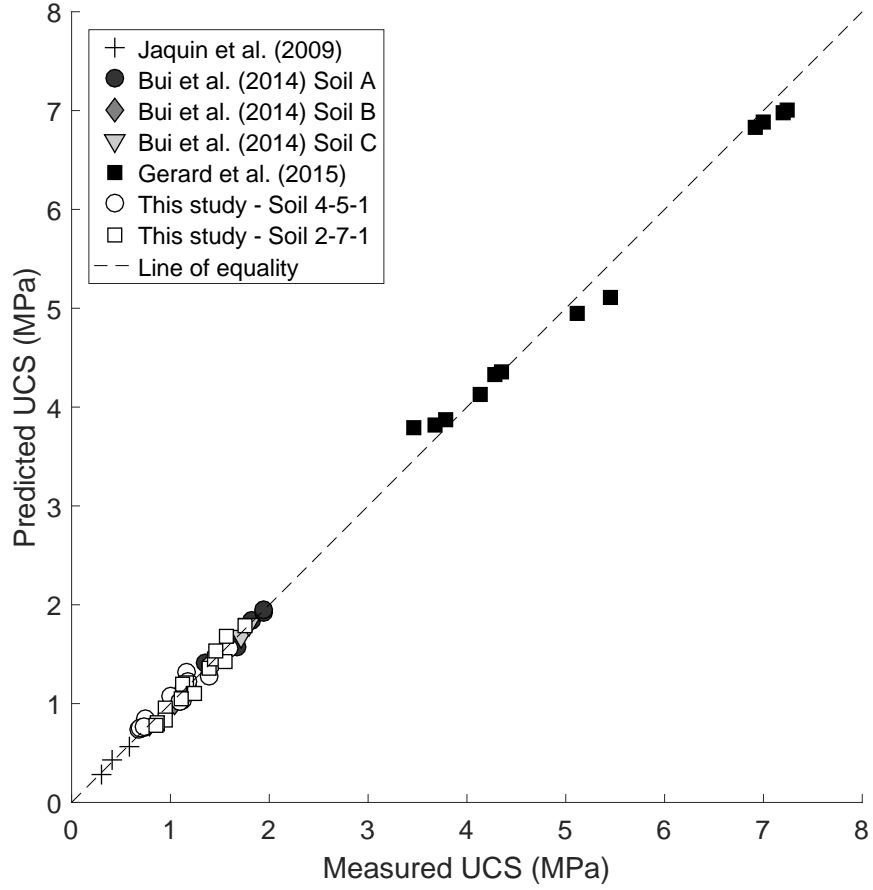


Figure 9: Measured and predicted UCS values for literature soil data

Table 4: EMC parameters derived for literature soils

Soil	$c'$ (kPa)	$\phi'$ ( $^{\circ}$ )	$\phi^b$ ( $^{\circ}$ )	$\phi^b$ ( $^{\circ}$ , Eqn 9)	$\kappa$ (Eqn 9)	Suction range (MPa)
Jaquin et al. (2009)	83.1	11.42	10.62	10.62	0.09	0.18–0.80
Bui et al. (2014) Soil A	512.7	11.92	0.24	0.24	3.72	3.2–65
Bui et al. (2014) Soil B	267.7	11.34	1.03	1.04	0.93	3.2–11
Bui et al. (2014) Soil C	566.2	12.63	0.25	0.25	1.25	8.1–36
Gerard et al. (2015)	929.4	38.5	0.32	0.32	3.07	4.1–126

263 RE soil or can afford the cost and delay of a lengthy laboratory campaign. To be  
264 useful to RE industry, the EMC method discussed above can be simplified in three  
265 key areas: i) tangential plane selection; ii) plane fitting; iii) testing equipment.

### 266 5.1. Plane selection

267 A complex (and potentially subjective) step of the plane-fitting process is  
268 identifying the most accurate tangent to the Mohr's circles. An alternative to  
269 a tangential failure envelope is to draw the envelope passing through the circle  
270 maxima, as shown in Figure 10 where subscripts  $c$  and  $t$  denote compression  
271 and tension respectively (Fredlund and Rahardjo, 1993). The advantage of this  
272 approach is that only one point per circle need be identified for plane fitting.  
273 UCS can be predicted from fitted  $c'$ ,  $\phi^*$  and  $\phi^B$  values via

$$\text{UCS} = 2 \left( \frac{c' + \psi \tan \phi^B}{1 - \tan \phi^*} \right) \quad (11)$$

274 as derived in the Appendix. Note that  $\phi^* \equiv \phi'$  and  $\phi^B \equiv \phi^b$  in function for the  
275 failure envelope defined using circle maxima.  $\phi^* \neq \phi'$  and  $\phi^b \neq \phi^B$ , however they  
276 are similar for most soils (Powrie, 2008).

277 (Insert Figure 10 somewhere near here)

278 To examine the validity of the simplified approach, UCS values for Soils 4-  
279 5-1 and 2-7-1 were re-predicted using Eqn 11. Measured and predicted values  
280 are compared in Figure 11. As for Figure 8, distinctions were made between  
281 strengths at suctions above and below the maximum ITS suction. With the  
282 exception of one result for Soil 4-5-1, results fall largely between the line of  
283 equality and an overprediction of roughly 0.15 MPa. The simplified method  
284 is therefore no less accurate, within the confines of available results, than the



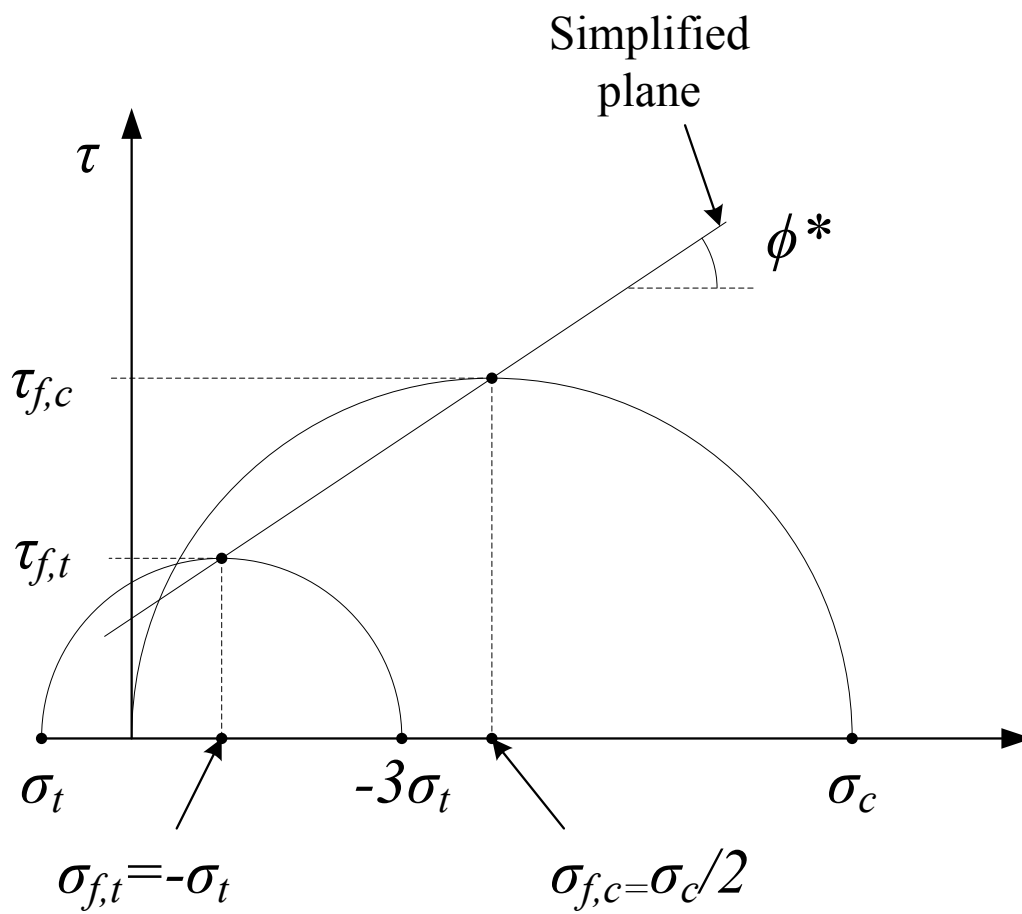


Figure 10: Construction of EMC failure envelope using circle maxima

285 full method. Strength overprediction is not conservative, however the amount is  
286 minor and can be accommodated by any reasonable margin of safety.

287 (Insert Figure 11 somewhere near here)

### 288 *5.2. Plane fitting*

289 Plane-fitting requires powerful computer software, for example MATLAB.  
290 That practitioners and laboratories will have access to such software or expertise  
291 in its use is unlikely. The fitting process can be significantly simplified by only  
292 testing specimens at the plane ‘corners’, i.e. performing UCS and ITS tests at  
293 the minimum and maximum anticipated suction conditions. That this is valid  
294 was demonstrated by the good agreement for predictions above the ITS suction  
295 limit in Figure 8.  $\phi^*$ ,  $\phi^B$  and  $c'$  calculations using this simplified method are  
296 derived in the Appendix. UCS can then be calculated using Eqn 11 as before.

### 297 *5.3. Testing equipment and revised experimental procedure*

298 Environmental chambers are large, expensive pieces of equipment and there-  
299 fore uncommon in most laboratories. An inexpensive alternative is to use satu-  
300 rated salt solutions to equilibrate specimens to target suction values. Potential  
301 solutions and corresponding suction values are given in Table 5 (Hall and Allinson,  
302 2009). Using this technique, a sealable container is partially filled with the salt  
303 solution and the specimen suspended above it until it reaches constant mass.  
304 Furthermore, the ITS ‘discs’ used here are not commonly encountered in prac-  
305 tice. Cylinders of the same dimensions used for UCS testing can be substituted  
306 for the discs;  $\sigma_t$  is given by Eqn 2 as before.

307 Based on these simplifications, an experimental procedure readily accessible  
308 and relevant to practitioners can be outlined:

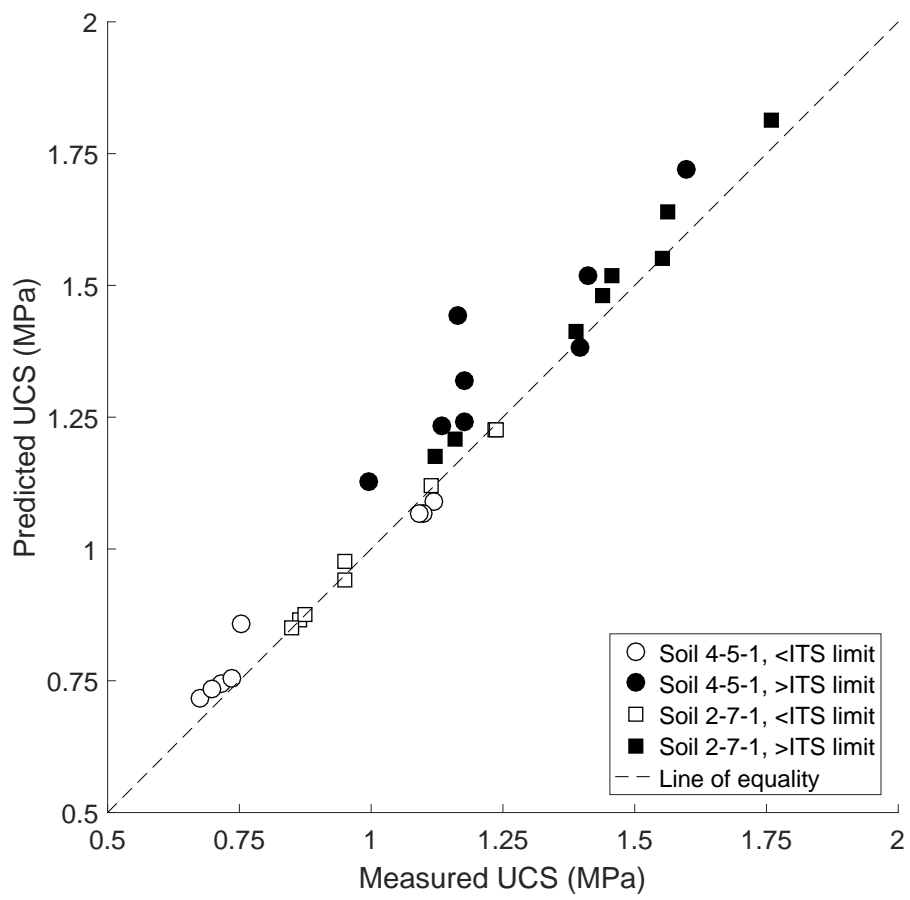


Figure 11: Comparison of measured and predicted UCS values found using the simplified EMC method

Table 5: Saturated salt solutions, associated RH and equivalent suction values for specimen suction equilibration (Hall and Allinson, 2009)

Salt solution	RH at 23°C	Suction (MPa)
Magnesium chloride	32.9±0.2	203.2
Potassium chloride	43.2±0.4	153.4
Magnesium nitrate	53.5±0.2	114.3
Sodium bromide	58.2±0.4	98.9
Sodium chloride	75.4±0.1	51.6
Potassium nitrate	94.0±0.6	11.3

- 309 1. Determine optimum compaction conditions for the proposed soil using stan-  
310 dard testing methods (e.g. AS1289, BS1377 etc.).
- 311 2. Obtain ambient site RH and  $T$  data (e.g. from government meteorological  
312 agencies) and calculate likely minimum and maximum suction conditions  
313 using Eqn 1.
- 314 3. Identify suitable salt solutions for this suction range (Table 5).
- 315 4. Manufacture three specimens (at the optimum compaction conditions) per  
316 suction condition for UCS and ITS testing.
- 317 5. Seal specimens in containers and periodically check mass until it becomes  
318 constant.
- 319 6. Test specimens for UCS or ITS using methods described in this paper. UCS  
320 or ITS is the average of the three specimen strengths.
- 321 7. Calculate  $c'$ ,  $\phi^*$  and  $\phi^B$  using simplified EMC method (Eqns 20 to 28).
- 322 8. Use EMC parameters to predict strengths for suction range of interest  
323 (Eqn 11).

#### 324 5.4. Implementation of simplified testing programme

325 To test its flexibility, the simplified testing programme outlined above was  
326 implemented at an RE construction facility (Watershed Materials) in California,

327 USA.  $\varnothing 150 \times 300$ mm UCS and ITS specimens were manufactured from a local  
328 rock aggregate, modified with 25% “C-Red” clay by mass (LL 24.1%, PL 16.2%,  
329 predominantly kaolinitic with a high iron content). Cylindrical specimens were  
330 selected for consistency with preferred industry practice. The final material’s par-  
331 ticle grading curve is shown in Figure 12. OWC (7.8%) and  $\rho_{d,max}$  (2100kg/m<sup>3</sup>)  
332 were determined following ASTM-D1557. Specimens were equilibrated at high  
333 and low humidities (93% and 34%) at 20°C, equivalent to 9.81 and 145.9 MPa  
334 suction respectively, using the above techniques, and tested in either compres-  
335 sion or tension on reaching constant mass. Three specimens were prepared per  
336 condition (12 in total).

337 (Insert Figure 12 somewhere near here)

338 To test the procedure’s ability to successfully predict strength across the suc-  
339 tion range, a failure plane was fitted to ITS results and UCS results at low suction  
340 only (i.e. using only three of the four ‘corners’ to define the plane). UCS and  
341 ITS results and the best-fitted failure plane to the selected Mohr’s circles (using  
342 circle maxima) are shown in Figure 13. EMC parameters are given in Table 6;  
343  $c'$ ,  $\phi^*$  and  $\phi^B$  values were similar to equivalent parameter values found for Soils  
344 4-5-1 and 2-7-1, likely due to the similar soil textures, densities and suction range.  
345 Agreement between the two indicated that the simplified procedure was able to  
346 capture reliable and representative EMC parameters; in the absence of a SWRC,  
347 however,  $\phi^B$  predictions using Eqn 9 could not be made. Strengths predicted  
348 from the restricted dataset are compared to those found by fitting a plane to all  
349 available data in Figure 14. As expected, excellent agreement was found between  
350 predicted and measured values using the full dataset due to the fitting nature of  
351 the procedure. Using the restricted dataset, predicted strengths were, at most,  
352 0.1MPa higher than measured values, i.e. within the anticipated accuracy found

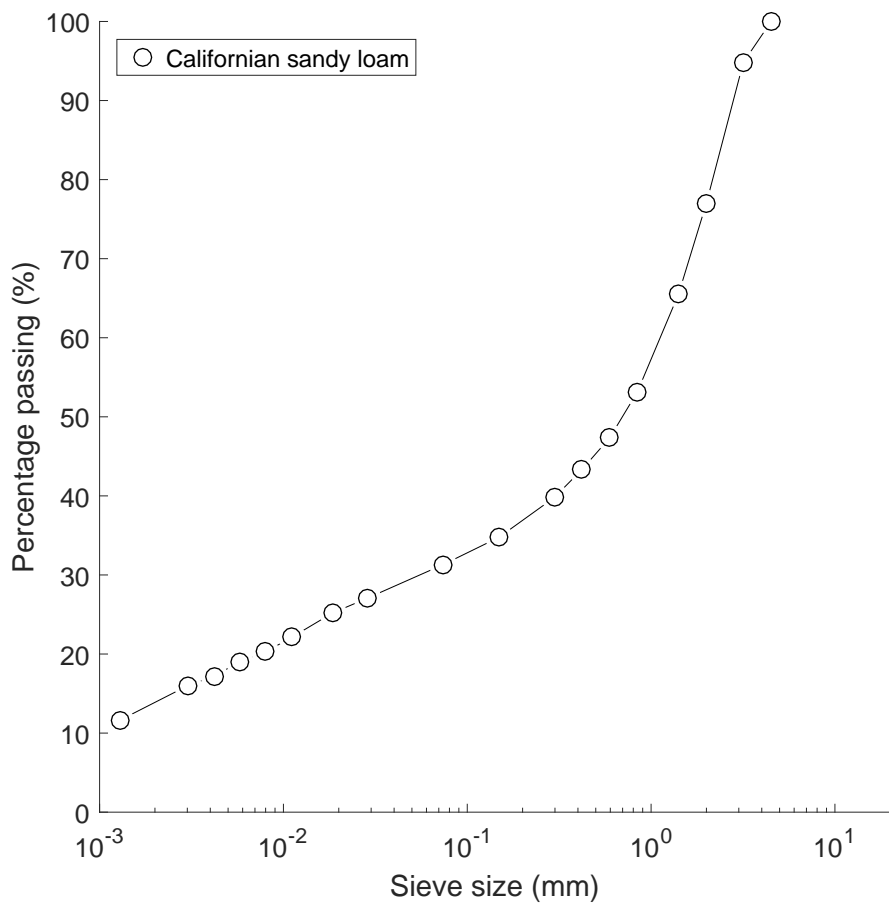


Figure 12: Particle grading curve for modified Californian sandy loam

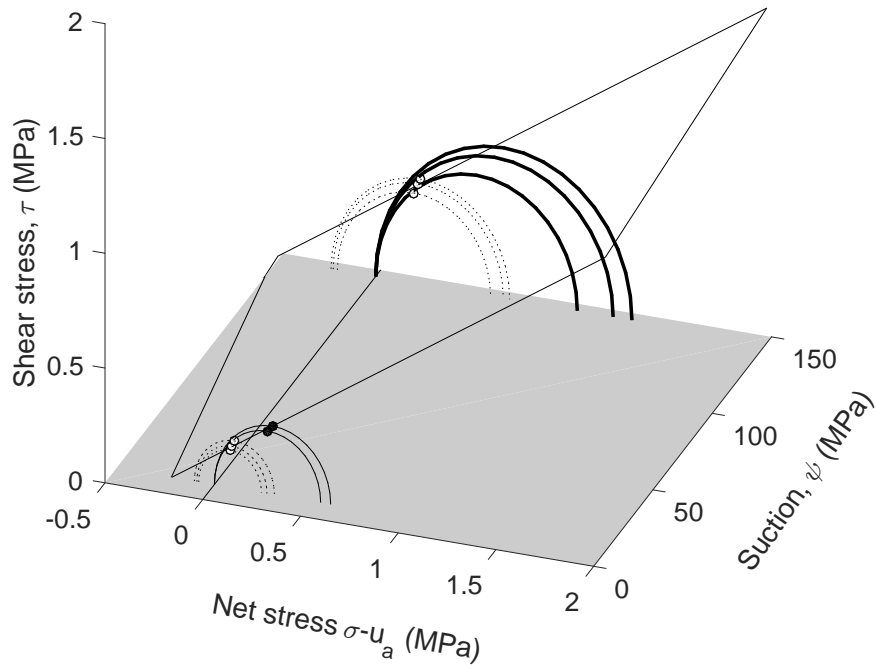


Figure 13: Planar EMC failure envelope for the Californian sandy loam. - UCS results; - - ITS results. Markers denote points on the circles used for plane fitting. Bold circles were omitted from plane-fitting for comparison to predicted values. Note that one UCS specimen at low suction was damaged prior to testing and so was not included

353 for the full procedure.

354 (Insert Figure 13 somewhere near here)

355 (Insert Figure 14 somewhere near here)

## 356 6. Conclusions

357 Strength uncertainty is a critical obstacle preventing RE's use in wider engi-  
 358 neering and construction practice. Recent research has demonstrated that suction

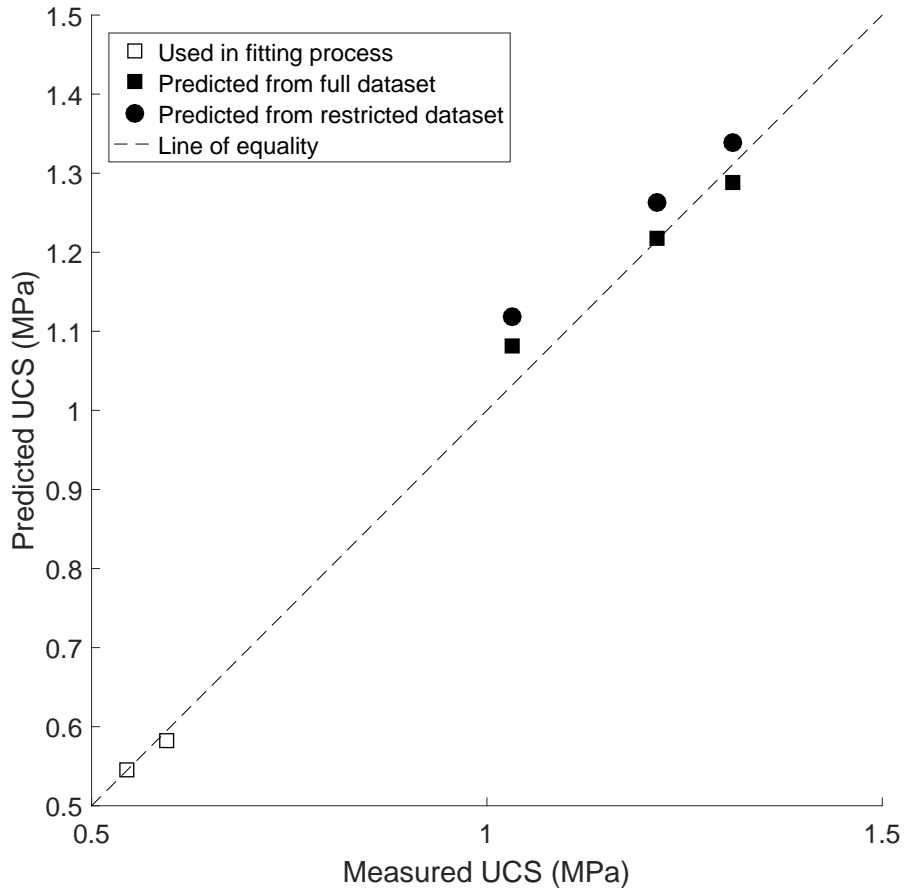


Figure 14: Comparison of measured and predicted UCS values for the Californian sandy loam found using the simplified EMC method and a restricted or complete dataset

Table 6: EMC parameters derived for the Californian sandy loam using the restricted and full dataset

Soil	$c'$ (kPa)	$\phi'$ ( $^{\circ}$ )	$\phi^b$ ( $^{\circ}$ )	Suction range (MPa)
Restricted dataset	112.7	30.0	0.075	9.81–145.9
Full dataset	128.6	25.9	0.073	9.81–145.9



359 is a key element controlling strength development in these materials. Developing  
360 a technique to reliably and realistically characterise strengths is key to improving  
361 confidence in RE design, construction and conservation programmes.

362 This paper presents suction-controlled UCS and ITS results for soils repre-  
363 sentative of the range and mineralogies likely to be used for RE construction.  
364 Strengths were found to almost double between the lowest and highest suctions  
365 for both soils. The EMC method was introduced to describe and predict strength  
366 changes with suction. Construction of the failure envelope was discussed and the  
367 use of a planar failure envelope in the residual suction range justified. Using  
368 this technique, good agreement ( $\pm 0.15$  MPa) was found between measured and  
369 predicted strengths for both tested soils across the entire suction range. Good  
370 agreement was also found when the technique was applied to literature data of  
371 varying suction ranges. Simplifications to the failure plane selection, fitting and  
372 experimental techniques were identified to adapt the developed technique to suit  
373 RE practice. The simplified plane selection and fitting techniques were tested on  
374 UCS and ITS data with no demonstrable loss in accuracy. Finally, the simplified  
375 experimental procedure was used to investigate strengths of a compacted Cali-  
376 fornian sandy loam tested at an existing RE construction facility. The simplified  
377 technique successfully predicted strengths over the entire suction range with the  
378 same accuracy as found for the full method.

### 379 **Acknowledgements**

380 The first author was supported by a studentship awarded by the School of  
381 Engineering and Computing Sciences, Durham University whilst this research  
382 was undertaken and is now supported by ARC Linkage Grant LP140100375.

383 **References**

- 384 ASTM, 2010. ASTM D5298-10. Standard test method for measurement of soil potential (suction)  
385 using filter paper.
- 386 Beckett, C. T. S., Augarde, C., 2012. The effect of relative humidity and temperature on the  
387 unconfined compressive strength of rammed earth. In: Mancuso, C., Jommi, C., D'Onza,  
388 F. (Eds.), *Unsaturated Soils: Research and Applications*. Second European Conference on  
389 Unsaturated Soils. Springer Berlin Heidelberg, pp. 287–292.
- 390 Beckett, C. T. S., Smith, J. C., Ciancio, D., Augarde, C. E., 2015. Tensile strengths of flocculated  
391 compacted unsaturated soils. *Géotechnique Letters* 5 (4), 254–260.
- 392 BSI, 1990. BS 1377:1990. Methods of testing for soils for civil engineering purposes.
- 393 Bui, Q.-B., Morel, J.-C., Hans, S., Walker, P., 2014. Effect of moisture content on the mechanical  
394 characteristics of rammed earth. *Construction and Building Materials* 54, 163–169.
- 395 Ciancio, D., Beckett, C. T. S., Carraro, J., 2014. Optimum lime content identification for lime-  
396 stabilised rammed earth. *Construction and Building Materials* 53, 59–65.
- 397 Fredlund, D., Rahardjo, H., 1993. *Soil mechanics for unsaturated soils*. John Wiley & Sons Inc.,  
398 New York (USA).
- 399 Fredlund, D. G., Morgenstern, N. R., 1977. Stress state variables for unsaturated soils. *Journal*  
400 *of the Geotechnical Engineering Division* 107 (GT5), 447–466.
- 401 Fredlund, D. G., Rahardjo, H., Gan, J. K.-M., 1–4 December 1987. Non-linearity of strength  
402 envelope for unsaturated soils. In: *Proceedings of the 6th International Conference on Ex-*  
403 *pansive Soils*. New Delhi, India, pp. 49–54.
- 404 Fredlund, D. G., Xing, A., 1994. Equations for the soil-water characteristic curve. *Canadian*  
405 *Geotechnical Journal* 31 (4), 521–532.
- 406 Fredlund, D. G., Xing, A., Fredlund, M. D., Barbour, S. L., 1996. The relationship of the  
407 unsaturated soil shear strength functions to the soil-water characteristic curve. *Canadian*  
408 *Geotechnical Journal* 32, 440–448.
- 409 Frydman, S., 1964. The applicability of the Brazilian (indirect tension) test to soils. *Australian*  
410 *Journal of Applied Science* 15 (4), 335–343.
- 411 Gan, J. K. M., Fredlund, D. G., Rahardjo, H., 1988. Determination of the shear strength  
412 parameters of an unsaturated soil using the direct shear test. *Can. Geotech. J.* 25 (3), 500–  
413 510.

- 414 Gerard, P., Mahdad, M., McCormack, A. R., François, B., 2015. A unified failure criterion for  
415 unstabilized rammed earth materials upon varying relative humidity conditions. *Construction*  
416 *and Building Materials* 95, 437–447.
- 417 Hall, M., Allinson, D., 2009. Analysis of the hygrothermal functional properties of stabilised  
418 rammed earth materials. *Building and Environment* 44 (9), 1935–1942.
- 419 Hall, M., Djerbib, Y., 2004. Moisture ingress in rammed earth: Part 1 - the effect of soil particle-  
420 size distribution on the rate of capillary suction. *Construction and Building Materials* 18 (4),  
421 269–280.
- 422 Hamblin, A. P., 1981. Filter paper method for routine measurement of field water potential.  
423 *Journal of Hydrology* 53 (3/4), 355–360.
- 424 Houben, H., Guillaud, H., 1996. *Earth construction - a comprehensive guide.*, Second Edition.  
425 Intermediate Technology Publications, London (UK).
- 426 Jaquin, P. A., Augarde, C. E., Gallipoli, D., Toll, D. G., 2009. The strength of unstabilised  
427 rammed earth materials. *Géotechnique* 59 (5), 487–490.
- 428 Khalili, N., Khabbaz, M. H., 1998. A unique relationship for  $\chi$  for the determination of the  
429 shear strength of unsaturated soils. *Géotechnique* 48 (6), 681–687.
- 430 Li, D., Wong, L. N. Y., 2013. The Brazilian disc test for rock mechanics applications: Review  
431 and new insights. *Rock Mechanics and Rock Engineering* 46 (2), 269–287.
- 432 McGregor, F., Heath, A., Maskell, D., Fabbri, A., Morel, J.-C., 2015. A review on the buffering  
433 capacity of earth building materials. *Construction Materials*.
- 434 NZS, 1998. NZS 4297:1998. Engineering design of earth buildings.
- 435 Panayiotopoulos, K. P., 1996. The effect of matric suction on stress-strain relation and strength  
436 of three alfisols. *Soil and Tillage Research* 39 (1-2), 45–59.
- 437 Powrie, W., 2008. *Soil Mechanics: Concepts and Applications*, 2nd Edition. Spon Press.
- 438 Standards Australia, 2003. AS1289.5.2.1.-2003. Methods of testing soils for engineering purposes.  
439 Method 5.2.1: Soil compaction and density tests Determination of the dry density/moisture  
440 content relation of a soil using modified compactive effort.
- 441 Vanapalli, S. K., Fredlund, D. G., Pufahl, D. E., Clifton, A. W., 1996. Model for the prediction  
442 of shear strength with respect to soil suction. *Can. Geotech. J.* 33 (3), 379–392.
- 443 Walker, P., Standards Australia, 2002. Hb 195: The Australian earth building handbook.

444 **Appendix**

445 *Full EMC strength prediction*

446 Derivation of Eqn 10 using Figure 15 for the full EMC method:

$$\tau_{f,pred} = c' + \sigma_{f,pred} \tan \phi' + \psi \tan \phi^b = \frac{\sigma_{c,pred}}{2} \cos \phi' \quad (12)$$

$$\sigma_{f,pred} = \frac{\sigma_{c,pred}}{2} (1 - \sin \phi') \quad (13)$$

447 Substitute Eqn 13 into 12 to find UCS,  $\sigma_{c,pred}$ :

$$\frac{\sigma_{c,pred}}{2} \cos \phi' = c' + \left( \frac{\sigma_{c,pred}}{2} (1 - \sin \phi') \right) \tan \phi' + \psi \tan \phi^b \quad (14)$$

$$\sigma_{c,pred} = 2 \left( \frac{c' + \psi \tan \phi^b}{\cos \phi' - (1 - \sin \phi') \tan \phi'} \right) \quad (15)$$

448 (Insert Figure 15 somewhere near here)

449 *EMC strength prediction using circle maxima*

450 Derivation of Eqn 11 using Figure 10 for the EMC method using circle max-  
451 ima:

$$\tau_{f,pred} = c' + \sigma_{f,pred} \tan \phi^* + \psi \tan \phi^B = \frac{\sigma_{c,pred}}{2} \quad (16)$$

$$\sigma_{f,pred} = \frac{\sigma_{c,pred}}{2} \quad (17)$$

452 Substitute Eqn 17 into 16 to find UCS,  $\sigma_{c,pred}$ :

$$\frac{\sigma_{c,pred}}{2} = c' + \left( \frac{\sigma_{c,pred}}{2} \right) \tan \phi^* + \psi \tan \phi^B \quad (18)$$

$$\sigma_{c,pred} = 2 \left( \frac{c' + \psi \tan \phi^B}{1 - \tan \phi^*} \right) \quad (19)$$

453 (Insert Figure 16 somewhere near here)

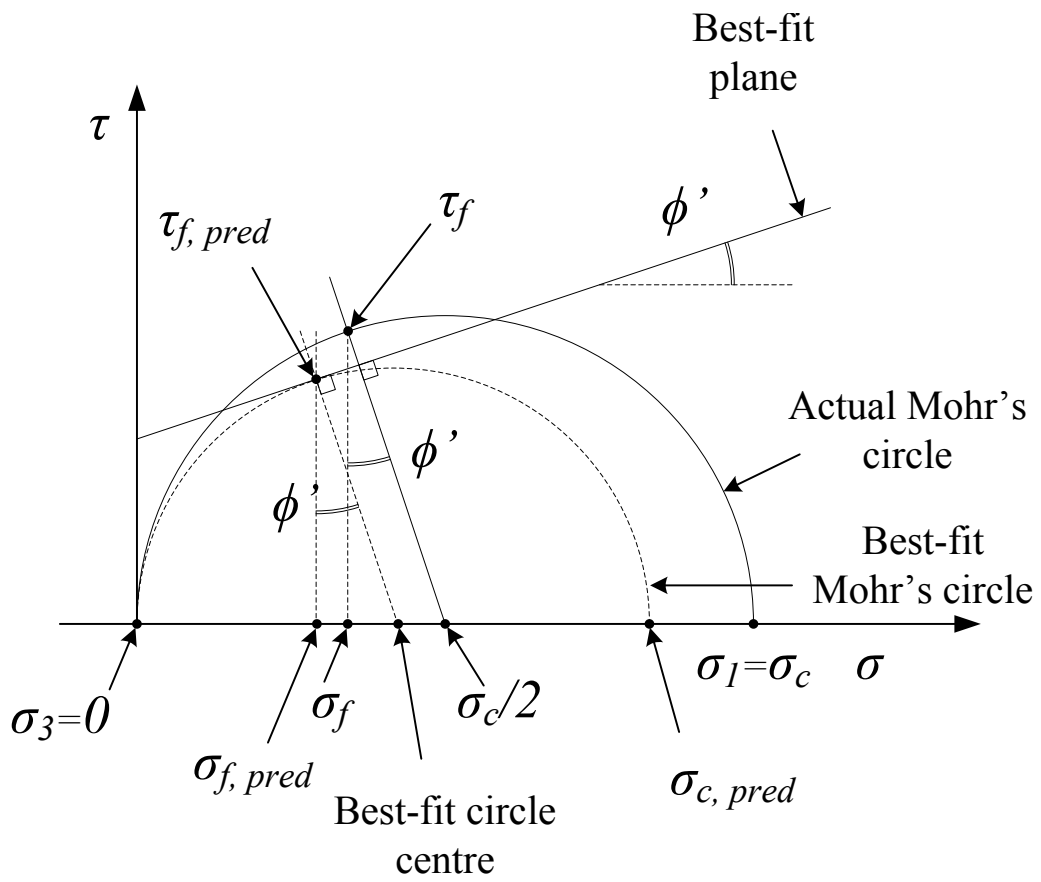


Figure 15: UCS calculation using full EMC method

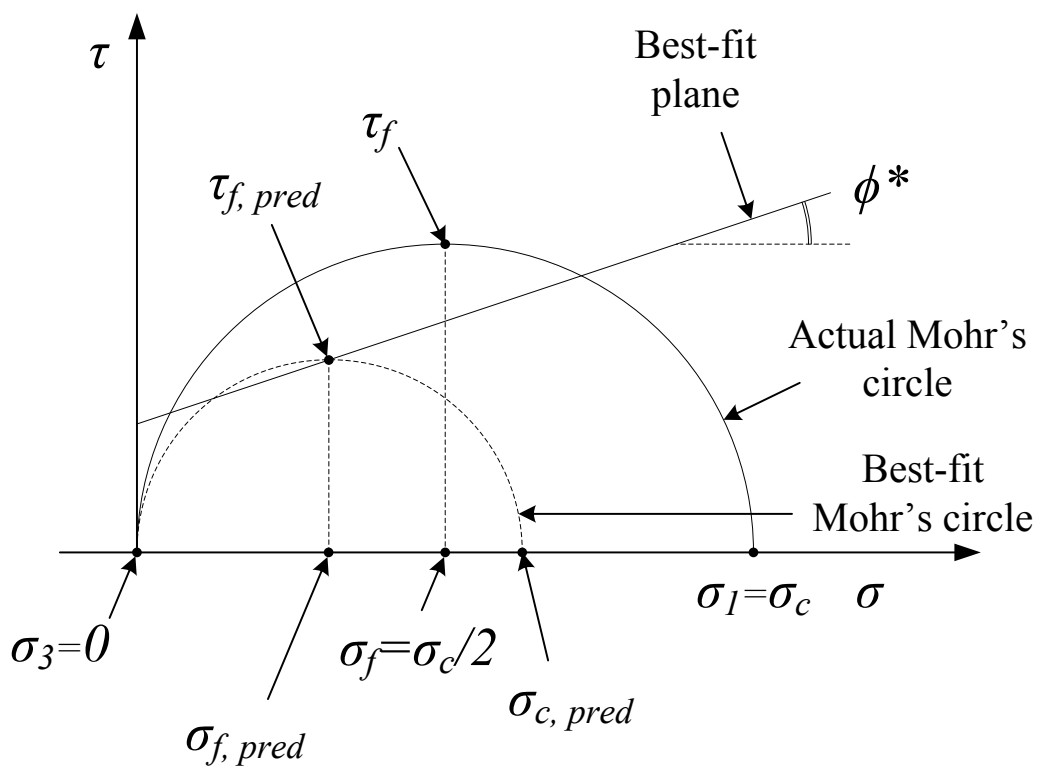


Figure 16: UCS calculation using full EMC method and circle maxima

454 *Simplified EMC strength prediction*

455 EMC parameter calculation using measured UCS and ITS values at plane  
456 corner points, using relationships shown in Figure 10:

$$\tan \phi_1^* = \frac{\sigma_{c1} + 4\sigma_{t1}}{\sigma_{c1} + 2\sigma_{t1}} \quad (20)$$

$$\tan \phi_2^* = \frac{\sigma_{c2} + 4\sigma_{t2}}{\sigma_{c2} + 2\sigma_{t2}} \quad (21)$$

$$\tan \phi^* = \frac{\tan \phi_1^* + \tan \phi_2^*}{2} \quad (22)$$

$$\tan \phi_c^b = \frac{\sigma_{c2} - \sigma_{c1}}{2(\psi_2 - \psi_1)} \quad (23)$$

$$\tan \phi_t^b = \frac{2(\sigma_{t1} - \sigma_{t2})}{\psi_2 - \psi_1} \quad (24)$$

$$\tan \phi^b = \frac{\tan \phi_c^b + \tan \phi_t^b}{2} \quad (25)$$

457 where  $\sigma_c$  and  $\sigma_t$  are measured UCS and ITS values, subscripts  $t$  and  $c$  stand for  
458 tension and compression and subscripts 1 and 2 indicate the lower and upper  
459 suction values respectively.  $c'$  can be solved by rearranging Eqn 11:

$$c'_1 = \frac{\sigma_c(1 - \tan \phi^*)}{2} - \psi \tan \phi^B \quad (\text{at } \psi_1) \quad (26)$$

$$c'_2 = \frac{\sigma_c(1 - \tan \phi^*)}{2} - \psi \tan \phi^B \quad (\text{at } \psi_2) \quad (27)$$

$$c' = \frac{c'_1 + c'_2}{2} \quad (28)$$

460 Note that  $\sigma_t$  is negative in Eqns 20 to 28.